ELSEVIER

Aspiration efficiency of a thin-walled probe at right angles to the wind

Laurie A. Brixey[1], Douglas E. Evans[2], James H. Vincent*

Department of Environmental Health Sciences, School of Public Health, University of Michigan, Ann Arbor, MI 48109, USA

Abstract

A new experimental system was recently developed for the rapid acquisition of data for aerosol sampler aspiration efficiency, and was applied in this latest work to the experimental study of thin-walled probes oriented at 90° to the freestream. Previous experimental studies from the 1980s, backed up by a physical model, suggested that aspiration efficiency for this orientation (A_{90}) may be uniquely described as a function of $St\,R^{1/2}$ (where St is the Stokes number for particle motion in the region of the sampler entry, and R is the ratio of the freestream air velocity to the average air velocity across the plane of the sampler inlet). But in this new work the experimental system was sufficiently selective as to allow detection of an additional dependency on R not revealed by the previous work. It is proposed that this additional dependency is associated with effects associated with the non-uniformity of the airflow distribution across the plane of the test sampler at such extreme orientations, derived from the inertia of the air motion as it approaches the sampler. One result of such non-uniformity is to reduce the effective cross-sectional area of the inlet as R increases. The experimental results suggest that A_{90} is now better described as a unique function of $St\,R^{1/4}$ (instead of $St\,R^{1/2}$). Such new insights into the basic physical behavior of a simple aerosol sampling scenario may be useful in helping to explain some aspects of the performances of more complicated aerosol samplers like those used in practical occupational and environmental air sampling situations.
© 2005 Elsevier Ltd. All rights reserved.

Keywords: Aerosol samplers; Thin-walled probes; Aspiration efficiency; Right angles

* Corresponding author. Tel.: +1 734 936 0703; fax: +1 734 936 7283.
 E-mail address: jhv@umich.edu (J.H. Vincent).
[1] Current affiliation: ManTech Environmental Technology, PO Box 12313, Research Triangle Park, NC, USA.
[2] Current affiliation: National Institute for Occupational Safety and Health, Cincinnati, OH, USA.

1. Introduction

The cylindrical thin-walled probe is perhaps the most idealized form of aerosol sampler. Due to its simplicity, it is one of the most extensively studied of all aerosol samplers. It remains important today because, by virtue of its relative simplicity, it offers insights into the fundamental nature of aerosol aspiration in much more complicated situations, including those pertaining to the collection of aerosols in ambient and working environments.

Most of the earlier published experimental data and theory on the performance of thin-walled, cylindrical probes (reviewed extensively in Vincent, 1989) were limited to the forwards-facing scenario and for relatively narrow ranges of so-called 'velocity ratio' (R), where R is defined as the ratio of the freestream air speed (U) to the mean speed of the air entering through the plane of the sampler entry (U_s). Indeed, the upper end of the range of R in those studies did not exceed about 5. More recently, however, research was conducted in our laboratory that extended R for thin-walled probes facing the wind up to close to 50 (Paik & Vincent, 2002).

When a cylindrical thin-walled probe is placed at angles to the wind other than forwards-facing, the physical scenario becomes more complicated. A smaller number of studies have addressed this more general case (Glauberman, 1962; Raynor, 1970; Lundgren, Durham, & Mason, 1978; Durham & Lundgren, 1980; Davies & Subari, 1982; Vincent, Stevens, Mark, Marshall, & Smith, 1986).

This paper is concerned with the special non-forwards-facing case in which the probe is placed at right angles to the freestream. This has previously been studied by Durham and Lundgren, Davies and Subari and Vincent et al., as cited above, as well as by Tufto and Willeke (1982) and Stevens (1986). Here we present new experimental data for aspiration efficiency, for a wider range of R than in the previously reported studies, and using a new rapid measurement method (as previously described in Brixey, Paik, Evans, & Vincent, 2002). Initial progress towards the development of a method of this type was first reported by Ramachandran, Sreenath, and Vincent (1998). This therefore provides an extended range of scientific information which in turn can be used to further enhance understanding of aerosol sampling in the more complex scenarios of more practical relevance. Indeed, this work was carried out in the context of the development of new, cost-effective methods for the testing of aerosol samplers for applications in occupational hygiene situations, where an important feature was the identification of scaling laws by which to relate sampler performance across wide ranges of external wind, sampling flowrate, dimensional and particle size conditions (as reported in full by Vincent, Brixey, & Evans, 2003).

2. Theoretical background

Aspiration efficiency (A) is the efficiency with which particles are transported from the ambient atmosphere into the body of a sampler. For a cylindrical thin-walled tube, it is the ratio of the concentration of particles entering through the plane of the entry of the tube (c_s) to that in the undisturbed upstream air (c_0). It is determined by inertial considerations, and well-known to be a function of R (as defined above) and Stokes number (St) as defined by

$$St = \tau/\tau_d, \tag{1}$$

where τ is the particle relaxation time given by

$$\tau = d_{ae}^2 \gamma^*/18\eta \tag{2}$$

in which d_{ae} is the particle aerodynamic diameter, γ^* the density of water (10^3 kg/m^3) and η the viscosity of air. When the tube is facing directly into the wind, τ_d in Eq. (1) is the time scale associated with the air flow distortion close to the sampler inlet, as expressed by

$$\tau_d = d/U \tag{3}$$

in which d is the sampler orifice diameter and U is the windspeed as already defined, and the nature of the distortion is such that—depending on the relative magnitudes of U and U_s—the flow approaching the entry is either convergent or divergent. For a thin-walled tube facing directly into the wind, it is easily shown that

$$A = 1 + \alpha(R - 1) \tag{4}$$

in which α is an inertial term which in turn has been shown to be closely represented by

$$\alpha = 1 - [1/(1 + G\,St)] \tag{5}$$

and G is a constant coefficient, which according to Paik and Vincent (2002), follows

$$G = 2 + (0.62/R) - 0.9R^{0.1}. \tag{6}$$

Here the first two terms on the right-hand side represent the form proposed by Belyaev and Levin (1974) and the last term represents an extension added to account for a wider range of R than was originally studied. Eq. (4) is the basis of almost all theoretical descriptions of aspiration efficiency for thin-walled tubes facing into the wind.

For tube orientations other than forwards-facing, the same basic framework applies. But now it is necessary to allow for the fact that the flow must not only diverge or converge, but must also turn to pass through the entry. In one formulation, Vincent et al. (1986) began with the expression

$$A = 1 + \alpha^*(R\,\cos\,\theta - 1), \tag{7}$$

where θ is the angle of orientation of the sampler with respect to the wind. The $R\,\cos\,\theta$ term allows for the change in the area of the sampling orifice projected upstream and where the inertial term is modified (as represented by α^*) to allow for the combined, parallel effects of the converging/diverging and turning of the flow. In order to support the discussion that will follow later in this paper, the development of the Vincent et al. model is summarized here. It was proposed that the latter could be achieved by modifying τ_d in Eq. (1), thus

$$\tau_d = \frac{\tau_{d1}\tau_{d2}}{\tau_{d1} + \tau_{d2}} \tag{8}$$

with

$$\tau_{d1} = \frac{d}{U\,\cos\,\theta} \quad \text{for divergence/convergence} \tag{9}$$

and

$$\tau_{d2} = \frac{z}{U} \quad \text{for turning.} \tag{10}$$

In the latter, z is the distance from the sampling orifice where the air velocity induced simply by the aspiration of air (i.e., no external wind) is the same as the component of the approaching freestream

parallel to the plane of the sampling orifice. We may approximate the sampling probe as a point sink and therefore estimate

$$4\pi z^2(U \sin \theta) = \pi d^2 U_s/4 \tag{11}$$

so that

$$\tau_{d2} = \frac{d}{4R^{1/2}U \sin^{1/2} \theta}. \tag{12}$$

By the insertion of Eqs. (2), (8), (9) and (12) in Eq. (1), we obtain

$$St_d = St\{\cos \theta + 4R^{1/2} \sin^{1/2} \theta\}. \tag{13}$$

The new equation for aspiration efficiency is now

$$A_\theta = 1 + \left[1 - \frac{1}{1 + G\,St(\cos \theta + 4R^{1/2} \sin^{1/2} \theta)}\right][R \cos \theta - 1] \tag{14}$$

which for $\theta = 90°$ reduces to

$$A_{90} = \frac{1}{1 + 4G\,St\,R^{1/2}} \equiv f\{G\,St\,R^{1/2}\}. \tag{15}$$

Similar functional forms have been developed by Tufto and Willeke (1982), Davies and Subari (1982) and Stevens (1986) and are broadly supported by the available experimental data (again see Vincent et al., 1986).

3. Experimental

3.1. Setup

The experiments described in this paper were carried out in a small open-loop wind tunnel that has been described fully elsewhere (e.g., Paik & Vincent, 2002; Brixey et al., 2002). It has a working cross-section of 30 cm × 30 cm, and air movement is driven by a tubular centrifugal fan located downstream of the working section. Air enters the working section from an inlet plenum containing a HEPA filter bank, a honeycomb screen and a contraction to suppress the penetration of external large-scale air motions into the working section. After passing through the working section, the air passes through a diffuser, and is discharged through another HEPA filter bank.

In our experiments, aerosolized powders of polydisperse glass beads (325 mesh, Class IV GL-0191 from MO-SCI Corp., Rolla, MO) were introduced into the wind tunnel upstream of the working section by means of a mechanical aerosol generator (Topas Model SAG 410, Topas GmbH, Dresden, Germany) for which the compressor-driven air supply was sufficient to provide an agglomerate-free aerosol. A square-mesh grid was located just downstream of the injection tube to facilitate mixing of the injected aerosol and to establish well-defined turbulence in the test section. The same conditions prevailed throughout all the experiments described. The full details can be found in the other reports cited above.

The central subject of this paper is application of a new method for the rapid testing of aerosol samplers first described by Brixey et al. It is based on use of the direct-reading Aerodynamic Particle Sizer (APS)

(Model 3321, TSI, Inc., St. Paul, MN) in a manner similar to the way it has been used by other researchers for the rapid experimental determination of aerosol penetration through cyclones and other particle size-selective media. By using polydisperse test aerosol, this approach can provide results for 52 electronic bins representing narrow particle size bands in the range of d_{ae} from approximately 0.5–20 μm within a single experimental run. The delivery rate of the aerosol generator was adjusted to provide aerosol concentration in the working section high enough to provide good particle counts across the range of particle sizes of interest yet not so high as to cause coincidence counts in the APS. With this in mind, the overall particle count concentration at the APS was maintained within the range from 50 to 400 particles/cm^3.

The APS data were acquired using Aerosol Instrument Manager software (Version 1.6, TSI, Inc., St. Paul, MN) on a laptop computer. Software was also compiled to control the collection of samples alternately and repeatedly through each of the reference and test sampling lines (see below). Individual sample duration was adjusted to obtain statistically sufficient total counts (> 100) in each channel, typically 90–120 s. Data records from each such run were exported to a spreadsheet (Microsoft Excel) that compared particle counts for the test sampler to the reference sampler and computed the average efficiency and associated statistical properties.

The APS requires a constant flowrate of 5 L/min, provided by an internal pump. In order for the test and reference samplers to sample at flowrates larger or smaller than 5 L/min, a tapered flow adapter was designed with additional ports to either add clean air or remove particle-laden air from the system. This was designed so that such addition or subtraction of air did not distort the flow field at the APS entry (Sreenath, 1998).

Finally, prior to each run, a check was carried out to examine the ratio of the particle counts, across the particle size range of interest, between the reference and test samplers, respectively, when the test sampler is oriented to face the wind. This provided information about how the incident aerosol concentrations differed between the upstream and downstream locations. The data that were obtained in this way provided the information needed to correct for such bias, and all the results presented in this paper have been thus corrected.

3.2. Approach

The new approach is embodied in Fig. 1. The actual experimental setup shown diagrammatically in Fig. 2 has been fully described elsewhere (Brixey et al., 2002) so the full technical details will not be repeated. The approach required measurement of the counts of particles of each given aerodynamic diameter reaching the APS in each of the two sampling lines shown, the first containing the reference sampler (subscript $_R$) where the aspiration characteristics are known and the second containing the actual sampling system of interest (subscript $_T$) where the aspiration characteristics are not known. The air volumetric flowrate was the same in each line. By repeated APS particle counts in each line, by switching backwards and forwards from one to the other, comparison of the counts obtained for each line provided information from which to determine the aspiration efficiency of the sampler of interest, in this case the thin-walled probe placed at 90° to the wind. By reference to Fig. 1, the aerosol penetration through the various parts of each line may be drawn together as follows:

$$\frac{_T c_{APS}}{c_0} = \frac{_T c_{APS}}{_T c_e} \frac{_T c_e}{_T c_s} \frac{_T c_s}{c_0} = {_T P_{tube}} \; {_T P_{entry}} \; {_T A}, \tag{16}$$
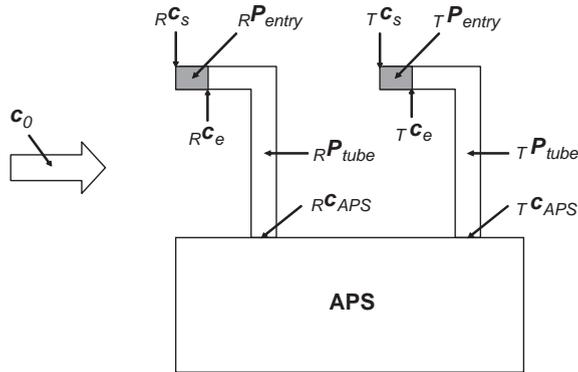
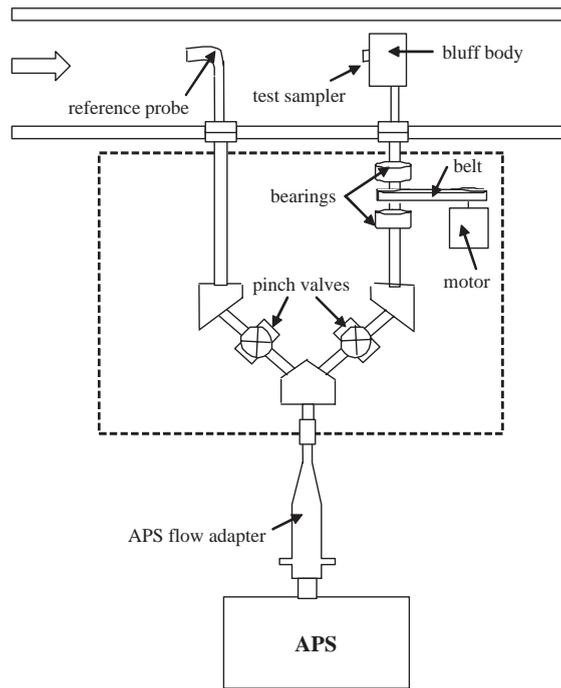Fig. 1. Conceptual summary of the experimental approach taken.

Fig. 2. Schematic drawing of the experimental setup.

$$\frac{{}_R c_{APS}}{c_0} = \frac{{}_R c_{APS}}{{}_R c_e} \frac{{}_R c_e}{{}_R c_s} \frac{{}_R c_s}{c_0} = {}_R P_{tube} \, {}_R P_{entry} \, {}_R A \tag{17}$$

leading to

$$\frac{{}_T c_{APS}}{{}_R c_{APS}} = \frac{{}_T P_{tube} \, {}_T P_{entry} \, {}_T A}{{}_R P_{tube} \, {}_R P_{entry} \, {}_R A}. \tag{18}$$
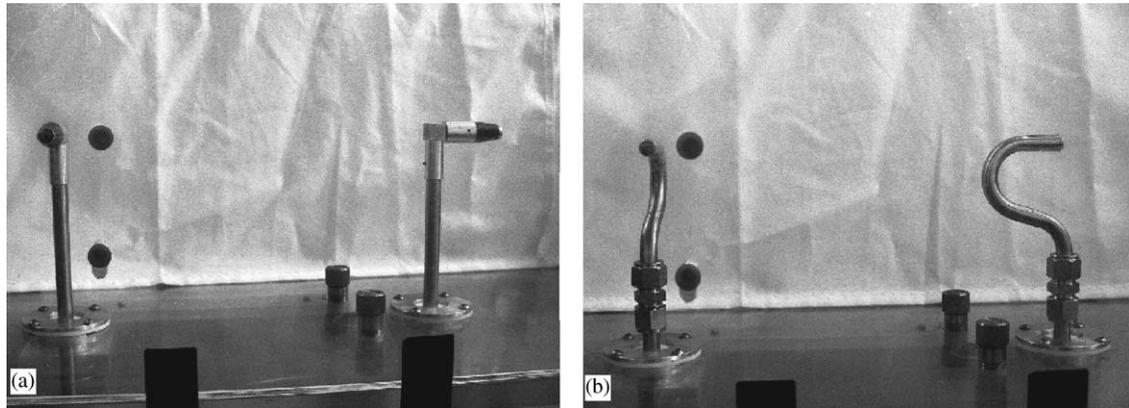
Fig. 3. Experimental setup for making aspiration efficiency measurements using: (a) 'straight' probes, and (b) 'goose-neck' thin-walled probes. In each case, the reference probe is on right, the test probe on the left, with the freestream moving from right to left.

In this scenario it is recognized that the flow in the entry region immediately behind the plane of the entry orifice is complicated by the coupling between the air outside and inside the sampling line. In particular, the boundary layer flow is strongly influenced by the relative air velocities in the freestream and plane of the entry, respectively, as well as by the orientation of the inlet. Sreenath et al. (2002) showed that this flow is so complicated that particle losses in this entry region cannot be predicted with any confidence. So here we have taken the approach that the problem should be eliminated as far as possible. To achieve this, short porous plastic foam plugs were inserted into the inlets of both the reference and the test probe. Such plugs have the effect that they straighten the flow entering through the inlet and eliminate the boundary layer effects—notably the *vena contracta*—that characterize the flow in the entry regions of the samplers. In addition, the efficiency of particle penetration through the entry region, shown in Fig. 1 and in the above equations as P_{entry}, can be predicted accurately using the model of Vincent, Aitken, and Mark (1993) (see also Kenny, Aitken, Beaumont, & Gorner, 2001). In this way, it can be arranged for the penetration efficiency for each of the foam plugs, $_{\text{T}}P_{\text{entry}}$ and $_{\text{R}}P_{\text{entry}}$, to be equal so that they cancel in Eq. (18). If in addition it is arranged that the corresponding lengths of tubing in the two sampling lines are also equal, then the aspiration efficiency for the test probe is given by

$$_{\text{T}}A \equiv A_{90} = \frac{_{\text{T}}c_{\text{APS}}}{_{\text{R}}c_{\text{APS}}}\,_{\text{R}}A. \tag{19}$$

Here, since $_{\text{R}}A$ may be determined for any set of operating conditions for the forwards-facing thin-walled reference probe using the thin-walled probe model of Paik and Vincent (2002), the only remaining unknown is the desired aspiration efficiency (A_{90}) for the test probe oriented at 90° to the wind.

3.3. Samplers

Two pairs of test samplers were designed for this study (see Fig. 3). The main body of experimental work was carried out using the 'straight' probes shown in Fig. 3a. A pair of 'goose-neck' samplers was later built (see Fig. 3b) after it was discovered early on in the work that there were intersampler biases

thought to be associated with small, but significant, differences in aerosol concentration across the wind tunnel working section (see below). All samplers had sharp, beveled entries and inlet diameter 11 mm. For the setup shown in Fig. 3a, the inlet of the straight test probe, when oriented at 90° to the wind, was located about 60 mm from the central axis of the wind tunnel. By contrast, for the setup shown in Fig. 3b the inlet of the goose-neck probe was located on the central axis of the wind tunnel for both the reference and the test probes.

As mentioned above, identical short plugs of porous plastic foam media were used to condition the air flow in the inlet region of each sampler. The foam media was obtained in 5 mm-thick sheets (Foam Engineers Ltd., Buckinghamshire, UK), and the grade chosen for our experiments was nominally 20 'pores per inch' (ppi), providing the desired flow conditioning while maintaining penetration efficiency across the range of particle size of interest large enough to allow sufficient particle counts at the APS. Prior to each experiment, the foam plugs for both the test and reference samplers were immersed in a 10% mixture of petroleum jelly in xylene and dried to leave a uniform greased surface that minimized re-entrainment of deposited particles. Preliminary experiments confirmed that greasing the foams in this way did indeed prevent such re-entrainment.

3.4. Procedures

Actual experimental determination of A_{90} using the preceding framework involved several steps. Aspiration efficiency values were calculated separately for each APS particle size bin, using Eq. (19) to produce an overall aspiration efficiency curve. In reality, in each given experimental run, the ratio $_T c_{APS} / _R c_{APS}$ was calculated for each of five actual samples by dividing each test sample, $_T c_{APS}$, by the average of the reference sampler values before and after the particular sample in question. For each run, therefore, eleven such particle counts were accumulated. In this way, for each set of experimental conditions, each sampling run provided five individual aspiration efficiency values for each particle size, yielding an average value and information about the statistical uncertainty in the experimental measurements reflecting in particular the variability of the aerosol concentration over time in the working section of the wind tunnel. For each set of experimental conditions we performed up to 10 separate such runs, so that a very large overall body of experimental data was accumulated.

4. Results

4.1. Preliminary experiments

A single set of results for the 90° thin-walled probe experiments using both the 'straight' and the corresponding 'goose-neck' probes is given in Fig. 4, plotted initially in the form of A_{90} versus *St* for the single value of $R = 2.75$. Here it is seen that the results for the straight probe contains a significant bias in that they do not approach unity as *St* becomes small, as should be the case from rudimentary physical considerations of the role of particle inertia. Similar biases were found for other *R*-values (not shown), tending to be greater for lower windspeeds. However, the corresponding results for the 'goose-neck' samplers do tend towards unity. These contrasting results are seen as clear evidence of the bias introduced by the spatial non-uniformity of the aerosol over the central region of the wind tunnel, small yet obviously significant. With this in mind, all the data obtained using the straight probes—representing the main body
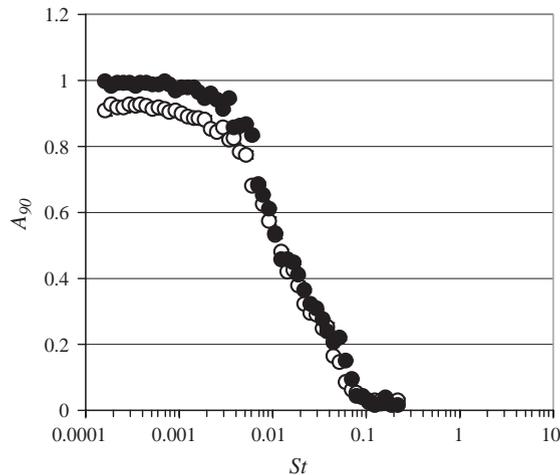
Fig. 4. Measured aspiration efficiency (A_{90}) for the straight (open circles) and goose-necked (closed circles) thin-walled sampling probes as a function of Stokes' number (St) for $R = 2.75$, showing the offset in A_{90} at small St for the straight probe.

of results presented in this paper—were corrected to force A_{90} to tend towards unity for small St. This was achieved by taking the average of the first eight aspiration efficiency values in each data set (for particle size bins representing the range $0.54\,\mu m < d_{ae} < 0.90\,\mu m$), and dividing the aspiration efficiency of the entire data set by this number.

4.2. Main experiments

A complete set of results, predominantly for the straight probe, corrected where appropriate, is shown in Fig. 5. Here, A_{90} is plotted against $St\,R^{1/2}$, for R-values of 2.75, 11 and 54.3, respectively. The error bars represent standard errors calculated from the repeat A_{90}-values. Overall the monotonic trend of A_{90} decreasing towards zero with increasing $St\,R^{1/2}$ is as expected from the theory outlined earlier. However, there are some additional trends not previously noted. Firstly, Fig. 5 reveals that there is an additional dependency on R not explained by $St\,R^{1/2}$. In addition, it is noted that there are large excursions from the main trend at larger values of $St\,R^{1/2}$, especially for $U = 3\,m/s$. The latter, however, are associated with the low particle counts that were experienced for certain experimental conditions, and so are not believed to have any physical significance.

5. Discussion

Fig. 5 also summarizes earlier results plotted in the same form by Vincent et al. (1986), which also included—in addition to their own experimental data—the previous results of Durham and Lundgren (1980) and Davies and Subari (1982) for the same experimental configuration. Those earlier results are represented in Fig. 5 by the envelope enclosed within the dotted line, and it is seen that agreement between these and our new results are generally good. In all those earlier experiments, each data point was obtained from a single, separate experiment carried out using a monodisperse test aerosol, and everything
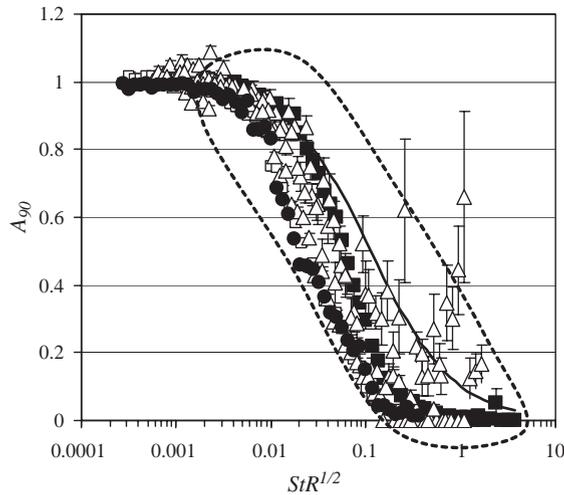
Fig. 5. Comparison of results for the thin-walled probe oriented at 90° to the wind plotted in the form of A_{90} versus $St\,R^{1/2}$ as suggested by Vincent et al. (1986), for $R = 2.75$ (closed circles), $R = 11$ (open triangles), $R = 54.3$ (closed squares); comparable previously published results are represented by the area enclosed by the dotted line; previously published semi-empirical model (——— Vincent et al., 1986).

passing through the plane of the sampler entry had been assessed. Therefore aspiration efficiency had been measured directly and unambiguously in all the results summarized by Vincent et al. (1986). The data set from Tufto and Willeke (1982) is also relevant, but is not included here because the experiments involved the use of direct-reading instrumentation, from which aspect it was similar to the present work, but the results had not been adjusted for inlet and sampling line losses. Overall, it is reasonable to suggest that the scatter for all the earlier studies was such that internal trends (i.e., the additional R-dependency) like those noted in the present work were not observable.

We now seek to explain the source of the additional R-dependency. The aspiration efficiency model described in Eqs. (1)–(15) is semi-empirical and describes fully the physical scenario quite accurately. It is also consistent with what has been proposed by others. Perhaps, therefore, it would be most profitable to focus attention on some of the assumptions that underlie the original model. One of them in particular is the assumption that the flow entering the sampler is uniformly distributed over the plane of the entry, and that the entry velocity U_s is fully described by

$$U_s = \frac{Q}{a} = \frac{4Q}{\pi d^2},\tag{20}$$

where Q is the volumetric sampling flowrate and a is the cross-sectional area of the entry. This is indeed a fair assumption for the samplers facing the wind. But it certainly will not be true for the tube at angles other than forwards-facing, where the *vena contracta* associated with the flow separation at the leading edge of the tube will distort the flow at the entry, the more so the larger the angle of the sampler orientation. As shown simplistically in Fig. 6a for 90° sampling, this will lead to a reduction in the effective area of the entry. It follows that U_s will be greater than stated in the model and, in turn, R will be smaller. For the foam-filled entry of the sampler that is the subject of the present research, it is expected—as originally intended—that the *vena contracta* effect will be absent. However, it is likely, as shown simplistically in
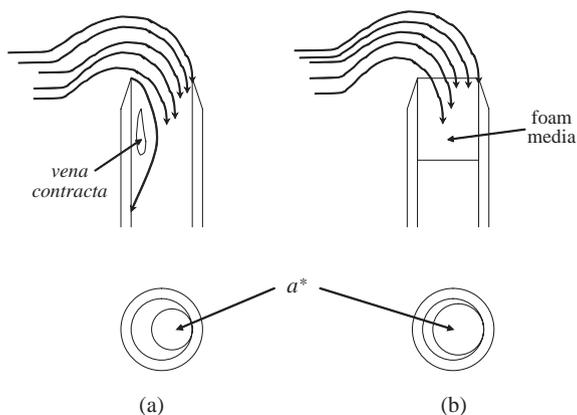
Fig. 6. Schematic drawings to illustrate (not to scale) the effect of inertia on the distribution of the airflow passing through the plane of the entry of the thin-walled probe for (a) the unmodified inlet, and (b) the inlet modified by the inclusion of a plug of porous plastic foam media.

Fig. 6b that the inertia of the flow will be such that the main airflow through the plane of the sampler entry will be biased towards the downstream side. Again, the effect will be to increase U_s and so reduce R.

The effect of these considerations leads to a re-think of how R appears in the model. Now a new quantity is suggested

$$R^* = \frac{U}{U_s^*} = \frac{U a^*}{Q} = R\frac{a^*}{a}, \tag{21}$$

where a^* is the new *effective* cross-sectional area of the entry, taking into account the inertia of the flow, and where $a^* < a$. It is reasonable to expect that

$$\frac{a^*}{a} = f(R). \tag{22}$$

There is no immediate theoretical basis for determining $f(R)$. So we must seek an empirical form that is physically plausible and satisfies what was observed experimentally. Inspection of the experimental results suggests

$$f(R) = R^{-1/2}. \tag{23}$$

This is plausible because it predicts that A^* will decrease as R increases (i.e., for higher external wind-speed), provided that $R > 1$.

Now, when R^* replaces R in Eq. (15), we get

$$A_{90} = \frac{1}{1 + 4G\,St(R^*)^{1/2}} = \frac{1}{1 + 4G\,St\,R^{1/4}} \equiv f\{G\,St\,R^{1/4}\}. \tag{24}$$

It is important to note that the bias we have identified will not be evident for the forwards-facing reference probe in our experiments. So Eq. (24) is a fair reflection of the experimental scenario we have described. It is also important to note that the inlet effect we have identified is equivalent to saying that $_R P_{entry}$ and $_T P_{entry}$ in Eq. (18) do not cancel after all.
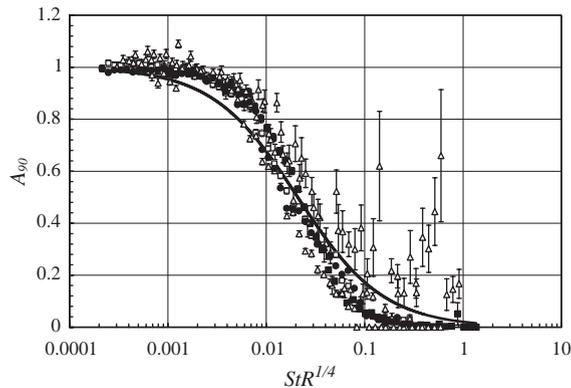
Fig. 7. Comparison of results for the thin-walled probe oriented at 90° to the wind plotted in the form of A_{90} versus $St\,R^{1/4}$ as suggested by the modified Vincent et al. (1986) model for $R = 2.75$ (closed circles), $R = 11$ (open triangles), $R = 54.3$ (closed squares). The solid curve represents the model shown in Eq. (24) with the coefficient $G = 12$.

With the preceding in mind, our results are plotted in the form of A_{90} versus $St\,R^{1/4}$ in Fig. 7 and it is seen that agreement with the new predicted trend is very good. Further, by placing $G = 12$ in Eq. (24), the model is seen to agree quantitatively quite well with the experimental results (see solid curve in Fig. 7). Although the exact form of the new model, as reflected in the exponent of R in Eq. (24), cannot be determined directly from physical arguments, it is satisfying that the general tendency is physically plausible, and that we have therefore gained a new insight into aerosol aspiration by a thin-walled probe oriented at angles away from the freestream.

6. Conclusions and implications

A new experimental system was previously developed for the rapid acquisition of data for aerosol sampler aspiration efficiency, and this has been applied in the present work to the study of thin-walled probes oriented at 90° to the freestream. Earlier experimental studies, backed up by a physical model, had suggested that A_{90} may be uniquely described as a function of $St\,R^{1/2}$. But the new experimental system was sufficiently selective as to allow a closer look at other trends that might be present, most notably an additional dependency on R not previously observed. It is suggested that this additional dependency derives from the non-uniformity of the airflow distribution across the plane of the test sampler at such extreme orientations, derived from the inertia of the air motion as it approaches the sampler. The result of such asymmetry is that the effective cross-sectional area of the inlet decreases as R increases. Based on this reasoning along with our new experimental results, A_{90} is better described as a unique function of $St\,R^{1/4}$.

From what we now know, the suggested air flow asymmetry across the plane of the sampling orifice will certainly be present for an entry that does not have a foam plug inserted just inside the entry. This indeed is a source of the entry loss for such sampling scenarios that had previously been identified by Ramachandran, Sreenath, and Vincent (2001). One implication of this latest finding is that the positioning of a foam plug inside the entry of a test sampler, either in this particular research or in other applications of the new method to other types of sampler, may not after all—as we had hoped—fully alleviate the

entry loss problem that Ramachandran et al. had identified earlier. There is a continued need, therefore, to take such considerations into effect in all experimental studies of aerosol sampler performance.

Acknowledgements

References

Belyaev, S. P., & Levin, L. M. (1974). Techniques for collection of representative aerosol samples. *Journal of Aerosol Science*, *5*, 325–338.

Brixey, L. A., Paik, S., Evans, D. E., & Vincent, J. H. (2002). Experimental studies to develop new aerosol samplers and methods for their evaluation. *Journal of Environmental Monitoring*, *4*, 633–641.

Davies, C. N., & Subari, M. (1982). Aspiration above wind velocity of aerosols with thin-walled nozzles facing and at right angles to the wind direction. *Journal of Aerosol Science*, *13*, 59–71.

Durham, M. D., & Lundgren, D. A. (1980). Evaluation of aerosol aspiration efficiency as a function of Stokes number, velocity ratio and nozzle angle. *Journal of Aerosol Science*, *11*, 179–188.

Glauberman, H. (1962). The directional dependence of air samplers. *American Industrial Hygiene Association Journal*, *23*, 235–239.

Kenny, L. C., Aitken, R. J., Beaumont, G., & Gorner, P. (2001). Investigation and application of a model for porous foam aerosol penetration. *Journal of Aerosol Science*, *32*, 271–285.

Lundgren, D. A., Durham, M. D., & Mason, K. W. (1978). Sampling of tangential flow streams. *American Industrial Hygiene Association Journal*, *39*, 640–644.

Paik, S., & Vincent, J. H. (2002). Aspiration efficiency for thin-walled nozzles facing the wind and for very high velocity ratios. *Journal of Aerosol Science*, *33*, 705–720.

Ramachandran, G., Sreenath, A., & Vincent, J. H. (1998). Towards a new method for experimental determination of aerosol sampler aspiration efficiency in small wind tunnels. *Journal of Aerosol Science*, *29*, 875–891.

Ramachandran, G., Sreenath, A., & Vincent, J. H. (2001). Experimental study of sampling losses in thin-walled probes at varying angles to the wind. *Aerosol Science and Technology*, *35*, 767–778.

Raynor, G. S. (1970). Variation in the entrance efficiency of a filter sampler with air speed, flow rate, angle and particle size. *American Industrial Hygiene Association Journal*, *31*, 294–304.

Sreenath, A. (1998). *On the physics of the aspiration process for blunt aerosol samplers*. Ph.D. thesis, University of Minnesota, MN, USA.

Stevens, D. C. (1986). Review of aspiration coefficients of thin-walled sampling nozzles. *Journal of Aerosol Science*, *17*, 729–743.

Tufto, P. A., & Willeke, K. (1982). Dependence of particulate sampling efficiency on inlet orientation and flow velocities. *American Industrial Hygiene Association Journal*, *43*, 436–443.

Vincent, J. H. (1989). *Aerosol sampling: Science and practice*. Chichester, UK: Wiley.

Vincent, J. H., Aitken, R. J., & Mark, D. (1993). Porous plastic foam filtration media: Penetration characteristics and applications in particle size-selective sampling. *Journal of Aerosol Science*, *24*, 929–944.

Vincent, J. H., Brixey, L. A., & Evans, D. E. (2003). *Methods for developing and testing aerosol samplers*. Final report on research carried out under NIOSH-CDC Grant No. 5 RO1-OH-02984-06.

Vincent, J. H., Stevens, D. C., Mark, D., Marshall, M., & Smith, T. A. (1986). On the aspiration characteristics of large-diameter, thin-walled aerosol sampling probes at yaw orientations with respect to the wind. *Journal of Aerosol Science*, *17*, 211–224.